

Scientific paper

Copper and Magnetic Activated Carbon Nanocomposites: Application as Recoverable Catalyst for C-S Coupling Reaction

Vajihe Nejadshafiee,^{1,2,*} Ehsan Ghonchepour,¹ Hojatollah Khabazzadeh,¹ Shahrzad Mahdavi Aliabad,¹ Fatemeh Hassani Bagheri¹ and Mohammad Reza Islami¹

1 Chemistry Department, Shahid Bahonar University of Kerman, Kerman 76169, Iran.

2 Central Lab, Vali-e-Asr University, 77176, Rafsanjan, Iran.

* Corresponding author: E-mail: nejadshafiee@sci.uk.ac.ir Tel: +98 034 31312200

Received: 08-13-2022

Abstract

In this study, activated carbon (AC) was prepared from pistachio nut shell precursor as agricultural by-product. The prepared AC was used to synthesize an efficient nanocomposite via loading of the copper metal and magnetic nanoparticles (Cu-MAC@C $_4$ H $_8$ SO $_3$ H NCs) onto its structure. The structure of the nanocatalyst was characterized by different methods such as FT-IR, TEM, EDS, XRD, VSM, and TGA analysis. The catalytic activity of the prepared composite was tested in a special C–S coupling, namely with the reaction of 2-mercapto-3-phenylquinazolin-4(3H)-one with iodobenzene or bromobenzene. The products of the aryl thioquinazoline derivatives were obtained in good yields and in short reaction times and the products were characterized with 1 H, 13 C NMR and CHNS analysis. On the other hand, with easy and high recovery of Cu-MAC@C $_4$ H $_8$ SO $_3$ H NCs through magnetic separation, a simple and green method to enhance the efficiency of the nanocatalyst has been provided. The nanocatalyst was reused in the next reaction in up to five cycles without obvious activity decrease.

Keywords: Magnetic nanoparticles, C-S coupling, green catalyst, quinazoline, activated carbon.

1. Introduction

According to the environmental movement of the 1960s, green chemistry prevents pollution by avoiding toxic and hazardous substances and minimizing waste in the production and application of chemical products. In recent years, chemists and engineers have been involved in the development of chemical products and processes that do not interfere with the environment or human health. The results of these research show that one of the fundamental pillars of green chemistry is the application of catalysts that can improve the chemical products and processes and reduce or eliminate the use and generation of hazardous substances. The fundamental properties of green catalysts are high stability, high activity, low preparation cost, great selectivity, easy and efficient recoverability and good recyclability. According to mentioned proper-

ties, heterogeneous catalysts can be good choice because they can be prepared via straightforward experimental procedures, they can be used under mild reaction conditions, their reusability is good and minimal waste disposal is needed.⁵⁻¹³ Two general strategies have been identified to facilitate catalyst recovery and reuse: the use of biphasic solvent systems and the use of heterogeneous or solid catalysts. 14 One of the most important factors in the preparation of solid catalysts is the supporting of catalyst by magnetic nanoparticles, which can be easily separated from the reaction mixture by an external magnet. Activated carbon has been included in various chemical processes such as adsorbent for adsorption processes and as a suitable solid bed for the preparation of heterogeneous catalysts in organic reactions due to its remarkable physical and chemical characteristics. 15-18 To improve the catalytic activity, recent studies have focused on supporting magnetic nanoparticles onto AC structure. By impregnating magnetic nanoparticles into AC, the characteristics of the resulting surface are modified so that there are a large number of active sites that can increase the catalytic capacity. ¹⁹ In particular, magnetic nanoparticles-loaded AC can be easily and quickly separated by using an external magnet.

Quinazoline is an aromatic heterocycle with a bicyclic structure consisting of two fused six-membered aromatic rings, a benzene ring and a pyrimidine ring. The synthesis of quinazoline compounds has received special attention from researchers because some quinazoline systems are biologically active and pharmaceutically useful, possessing antifungal, 20,21 anti-HIV,22 antiviral,23 antimalarial,24 anti-inflammatory,25 and antibacterial26 activities. For example, Gefitinib can bind to the ATP-binding site of EGFR, thus inactivating the anti-apoptotic Ras signal transduction cascade preventing further growth of cancer cells, and Lapatinib eliminates the growth of breast cancer stem cells that cause tumor growth, and Erlotinib binding to the ATP-binding sites of the EGFR receptors prevents EGFR from producing phosphotyrosine residues. 27-29

Herein, we report the preparation of modified magnetic activated carbon (MAC) with 1,4-butane sultone and copper (Cu-MAC@C $_4$ H $_8$ SO $_3$ H NCs). Then the nanocomposites were studied for their catalytic activity in C–S coupling reaction for the synthesis of aryl thioquinazoline derivatives and the results exhibited an excellent catalytic activity in the reaction. The nanocomposite structure was characterized systematically by different techniques such as FT-IR, TEM, EDX, XRD, VSM and TGA.

2. Experimental Section

2. 1. Materials

All solvents and reagents were directly used in analytical grade purity without further purification. All experiments were performed using deionized water (DI).

2. 2. Synthesis of MAC@C₄H₈SO₃H NCs

The dried pistachio nut shells were firstly crushed into dimensions 1–2 mm and carbonized at 700 °C for 1.5 h. Then, the carbon was activated under steam at 900 °C for 10 h duration. To increase the active sites on the AC, firstly, the AC (1.5 g) was stirred in HCl solution (0.05 M, 15 mL) for 48 h and then immersed into HNO $_3$ solutions (50%, then 69%) at 50 °C for 10 h, finally, the obtained AC was washed with the DI water three times and dried at 40 °C for 12 h.

Preparation of MAC: FeCl₃·6H₂O (50 mL, 0.3 M) was added to a dilute solution of HCl (0.5 mL, 0.2 M) and the reaction flask was placed in the ultrasonic probe and irradiated at 80 kHz for 5 min. Then Na_2SO_3 (20 mL, 0.3 M) was added into 40 mL of the above solution, after 5 min under ultrasound irradiation, the AC (1 g) was added to the reaction mixture. In the following, the resulting mix-

ture was poured to the solution containing water and ammonia (400 mL, 60 mL) and was sonicated for 30 min. Finally, the obtained magnetic dispersion was subjected to magnetic separation with a magnet, washed with water three times, and dried under vacuum at 60 °C for 12 h.

Preparation of MAC@C $_4$ H $_8$ SO $_3$ H NCs: compound 1,4-butane sultone (5.75 mmol) was added to a KCl solution (0.575 M) and was sonicated for 20 min. Then the dispersed MAC (0.2 g in EtOH (10 mL)) was added to the above mixture and the reaction was stirred for 4 h at 60 °C. After this time the reaction was continued for 10 h at room temperature. The magnetic product (MAC@C $_4$ H $_8$ SO $_3$ H NCs) was separated by an external magnet and washed with DI water and dried under vacuum in an oven.

2. 3. Synthesis of Cu-MAC@C₄H₈SO₃H NCs

The MAC@C $_4$ H $_8$ SO $_3$ H nanocomposite (0.5 g) was added to a mixture of 134 mg of copper(II) chloride and 50 mL solvent (H $_2$ O/MeOH 1:1). The mixture was continuously stirred for 24 h at room temperature. The final product (Cu-MAC@C $_4$ H $_8$ SO $_3$ H NCs) was separated by an external magnet and washed with DI water and dried under vacuum oven.

General Procedure for the Synthesis of Aryl Thioquinazoline Derivatives in the Presence of Cu-MAC@C₄H₈SO₃H NCs

To a solution of arylhalide compound (0.5 mmol), 2-mercapto-3-phenylquinazolin-4(3H)-one (0.5 mmol) and 0.75 mmol K₂CO₃ in 1.5 mL DMF was added, followed by 20 mg of the catalyst Cu-MAC@C₄H₈SO₃H. The mixture was heated and stirred at 110 °C for 4 h. The progress of the reaction was monitored by TLC. After 4 h, the nanoparticles were separated with an external magnet from the reaction mixture and washed with DI water and diethyl ether. Water (50 mL) was added to the reaction mixture and extracted with CH₂Cl₂ (2×25 mL) and dried over Na₂SO₄. The solvent was removed under reduced pressure to give the crude product. The residue was subjected to column chromatography using mixture of n-hexane and ethyl acetate as the eluent to afford pure product.

3-Phenyl-2-(phenylthio)quinazoline-4-(3*H***)-one (3a).** White solid, m.p. 149–152 °C. IR (KBr): 3057, 2921, 1691, 1626, 1541, 1465, 1295, 1257, 1202, 767 cm⁻¹, ¹H NMR (400 MHz, CDCl₃): δ 8.24 (s, 1H, ArH), 7.58–7.56 (m, 4H, ArH), 7.42–7.33 (m, 4H, ArH); ¹³C NMR (100 MHz, CDCl₃): δ 161.9, 157.1, 147.7, 136.0, 135.7, 134.4, 130.0, 129.7, 129.6, 129.3, 129.0, 128.6, 127.1, 126.7, 125.9, 119.9. Anal. calcd for C₂₀H₁₄N₂OS (330.40): C, 72.70; H, 4.27; N, 8.48; S, 9.70; found: C, 72.77; H, 4.55; N, 8.15; S, 9.88.

2-((4-Methoxyphenyl)thio-3-phenylquinazoline-4-(3*H*)-one (3*b*). White solid, m.p. 150–152 °C. IR (KBr):

3065, 1728, 1626, 1573, 1468, 1250, 1173, 690 cm⁻¹. 1 H NMR (400 MHz, CDCl₃): δ 8.22 (s, 1H, ArH), 7.63–7.61 (m, 3H, ArH), 7.60–7.58 (m, 2H, ArH), 7.45–7.42 (m, 4H, ArH), 7.37–7.352 (m, 2H, ArH), 7.45–7.42 (m, 4H, ArH), 6.95 (d, 1H, ArH), 3.85 (s, 1H, OCH₃); 13 C NMR (100 MHz, CDCl₃): δ 161.9, 160.7, 157.7, 147.7, 137.3, 135.9, 134.3, 129.9, 129.6, 129.2, 126.9, 125.8, 119.8, 119.1, 114.6, 55.3. Anal. calcd for $C_{21}H_{16}N_2O_2S$ (360.43): C, 69.98; H, 4.47; N, 7.77; S, 8.90; found: C, 69.84; H, 4.54; N, 7.97; S, 8.50.

3-Phenyl-2-(*p***-tolylthio)quinazoline-4-(3***H***)-one (3***c***). White solid, m.p. 151–153 °C. IR (KBr): 3066, 1682, 1573, 1464, 1256, 1197, 766 cm⁻¹. ¹H NMR (400 MHz, CDCl₃): δ 8.23 (s, 1H, ArH), 7.65–7.57 (m, 3H, ArH), 7.45–7.42 (m, 4H, ArH), 7.37–7.36 (m, 3H, ArH), 7.26–7.23 (m, 2H, ArH), 2.42 (s, 1H, CH₃); ¹³C NMR (100 MHz, CDCl₃): δ 162.1, 157.6, 147.9, 139.9, 136.2, 135.3, 130.1, 129.9, 129.4, 127.2, 126.8, 126.0, 120.1, 21.5. Anal. calcd for C_{21}H_{16}N_2OS (344.43): C, 73.23; H, 4.68; N, 8.13; S, 9.31; found: C, 72.99; H, 4.67; N, 8.23; S, 9.10.**

2-((4-Nitrophenyl)thio)-3-phenylquinazoline-4- (**3H)-one (3d).** Orange solid, m.p. 153–155 °C. IR (KBr): 3104, 2974, 2925, 1690, 1548, 1511, 1466, 1343, 1258, 1050, 769 cm⁻¹. ¹H NMR (400 MHz, CDCl₃): δ 8.27–8.25 (m, 2H, ArH), 8.23 (m, 1H, ArH), 7.76–7.74 (m, 2H, ArH), 7.68 (m, 1H, ArH), 7.62–7.61 (m, 2H, ArH), 7.44–7.42 (m, 4H, ArH), 7.37–7.35 (m, 1H, ArH); ¹³C NMR (100 MHz, CDCl₃): δ 161.0, 154.5,

147.7, 146.7, 136.5, 134.3, 135.0, 134.2, 129.8, 129.3, 128.6, 125.9, 123.2, 119.5. Anal. calcd for $C_{20}H_{13}N_3O_3S$ (344.43): C, 63.99; H, 3.49; N, 11.19; S, 8.54; found: C, 63.77; H, 3.44; N, 11.31; S, 8.84.

2-((4-Bromophenyl)thio)-3-phenylquinazoline-4- (*3H*)-one (*3e*). White solid, m.p. 154–156 °C. IR (KBr): 3067, 1695, 1549, 1466, 1260, 1110, 765 cm⁻¹. ¹H NMR (400 MHz, CDCl₃): δ 8.23 (m, 1H, ArH), 7.66–7.64 (m, 1H, ArH), 7.61–7.58 (m, 2H, ArH), 7.57–7.55 (m, 2H, ArH), 7.43–7.36 (m, 7H, ArH); ¹³C NMR (100 MHz, CDCl₃): δ 161.6, 156.2, 147.4, 137.0, 135.6, 132.0, 129.6, 129.0, 127.5, 126.9, 126.5, 125.9, 124.1, 119.8. Anal. calcd for C₂₀H₁₃BrN₂O₃S (409.30): C, 58.69; H, 3.20; N, 6.84; S, 7.83; found: C, 58.92; H, 3.24; N, 6.91; S, 7.55.

3. Results and Discussion

The synthesis of Cu-MAC@C $_4$ H $_8$ SO $_3$ H NCs catalyst, along with the growth of Fe $_3$ O $_4$ NPs and the loading of C $_4$ H $_8$ SO $_3$ H and copper onto AC is shown in Scheme 1.

3. 1. Characterization

FT-IR spectra were recorded on a commercial spectrophotometer (Bruker Tensor 27 FT -IR). ¹H and ¹³C NMR spectra were recorded on a Bruker 400 Ultrashield NMR Magnet (400 MHz for ¹H NMR) with TMS as the internal standard. Powder X-ray diffraction (XRD) spectra

Scheme 1. Synthesis steps of Cu-MAC@C₄H₈SO₃H NCs.

were recorded at room temperature with a Philips X-Pert 1710 diffractometer using Co Ka (λ = 1.78897 Å) at a voltage of 40 kV and a current of 40 mA and data were collected from 10° to 90° (20) with a scan speed of 0.02° s. The morphology of the catalyst was studied using scanning electron microscopy (SEM; Philips XL 30 and S-4160) with coated gold equipped with dispersive X-ray spectroscopy capability. Thermogravimetric analysis (TGA) and differential thermal analysis (DTA) were performed using a thermal analyzer with a heating rate of 20 °C/min in a temperature range of 25–1100 °C under flowing compressed nitrogen. The magnetic properties of the catalyst were measured with a vibrating sample magnetometer (VSM).

The FT-IR spectrum of the AC exhibits the bands corresponding to the functionalities containing hydroxyl OH group (~3442 cm⁻¹), carboxyl C=O group (~1719 cm⁻¹), C=C (~1577 cm⁻¹), C=O group (~1384 cm⁻¹) (Figure 1a). The presence of Fe=O band (~673 cm⁻¹) in the FT-IR spectrum of Fe₃O₄ NPs@AC confirms that the Fe₃O₄ NPs are located on the AC structure (Figure 1b). In the Figure 1C, the new bands observed at 2919 cm⁻¹ and 1036 cm⁻¹ due to the stretching vibrations of sp³ C=H and C=S bands respectively prove that 1,4-butane sultone was loaded on the MAC@C₄H₈SO₃H. Furthermore, the FT-IR spectrum of Cu-MAC@C₄H₈SO₃H NCs exhibits a new absorption band at 583 cm⁻¹ due to the presence of copper in the structure (Figure 1d).

Figure 2 illustrates the XRD patterns of AC, MAC and MAC@ $C_4H_8SO_3H$. A broad diffraction peak was obtained at $2\theta = 25.31^\circ$ for AC due to the plane of amorphous activated carbon. In XRD patterns of MAC, some peaks appeared at 30.51°, 35.81°, 43.51°, 54.15°, 57.46°, 63.06° and 74.60° related to the cubic spinel structure of magnetic

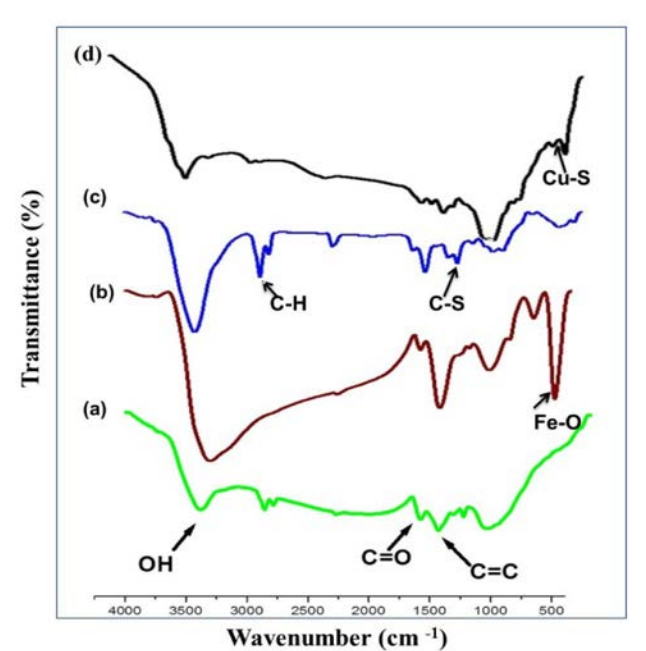


Figure 1. FTIR spectra of (a) AC, (b) MAC (c) MAC@C $_4$ H $_8$ SO $_3$ H and (d) Cu-MAC@C $_4$ H $_8$ SO $_3$ H NCs.

nanoparticles. The XRD pattern of MAC@ $C_4H_8SO_3H$ was almost similar to the MAC but the intensity of peaks decreased which could be related to immobilizing of $C_4H_8SO_3H$ onto MAC.

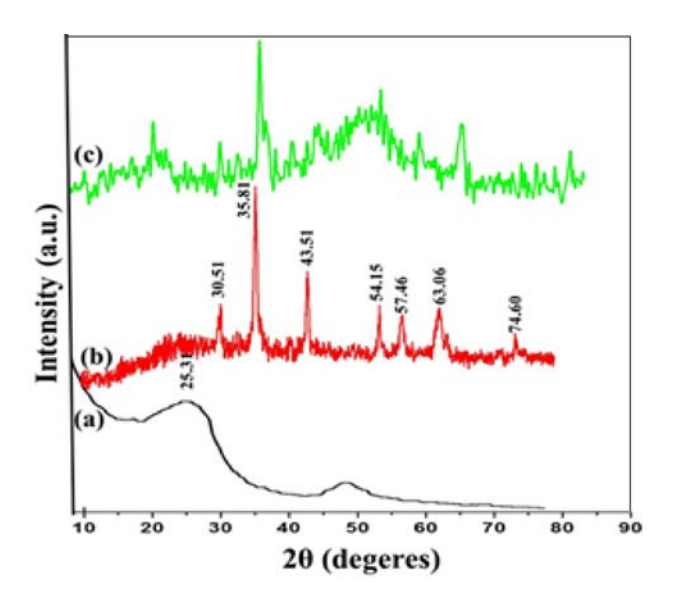


Figure 2. XRD patterns of (a) AC, (b) MAC and MAC@C₄H₈SO₃H.

The morphology of AC, MAC and MAC@C $_4$ H $_8$ SO $_3$ H were deduced by TEM analysis and the TEM images are shown in Figure 3. The mesoporous structure of AC was observed by TEM (Figure 3a). The TEM images of MAC and MAC@C $_4$ H $_8$ SO $_3$ H show that the Fe $_3$ O $_4$ nanoparticles are coated onto AC (Figures 3b–c). Figures 3b and c show that the particle size of MAC@C $_4$ H $_8$ SO $_3$ H is larger than MAC (from 30 to 50 nm, respectively), which could be due to the immobilization of 1,4-butane sultone onto the surface of the MAC.

Thermal stability was studied by thermal gravimetric analysis of AC, MAC, MAC@C4H8SO3H and Cu-MAC@C₄H₈SO₃H NCs (Figure 4). The thermal gravimetric analysis of AC displayed a weight loss below at temperatures of 175 °C, at 200-400 °C, and 500-750 °C, which could be ascribed to the loss of adsorbed water (15.43%), exclusion of oxygenated functional groups (8.85%), and ultimately to the decomposition of AC (72.48%), respectively (Figure 4a). The TGA curve of MAC showed a weight loss of about 51.14% (Figure 4b). For MAC@C₄H₈SO₃H a weight loss occurred at 160–350 $^{\circ}$ C about 4.45%, resulting from the pyrolysis of $C_4H_8SO_3H$ functional groups (Figure 4c). Also, about 40.0% of MAC and H₃NSO₃-MAC NCs retained at 750 °C, due to the remaining iron oxide. The TGA curve of Cu-MAC@ C₄H₈SO₃H showed an increase in temperature to 950 °C which is related to the coordination of Cu(II) ions with the active sites of MAC@C₄H₈SO₃H surface. Also, Cu-MAC@C₄H₈SO₃H retained about 64.0% of its weight at

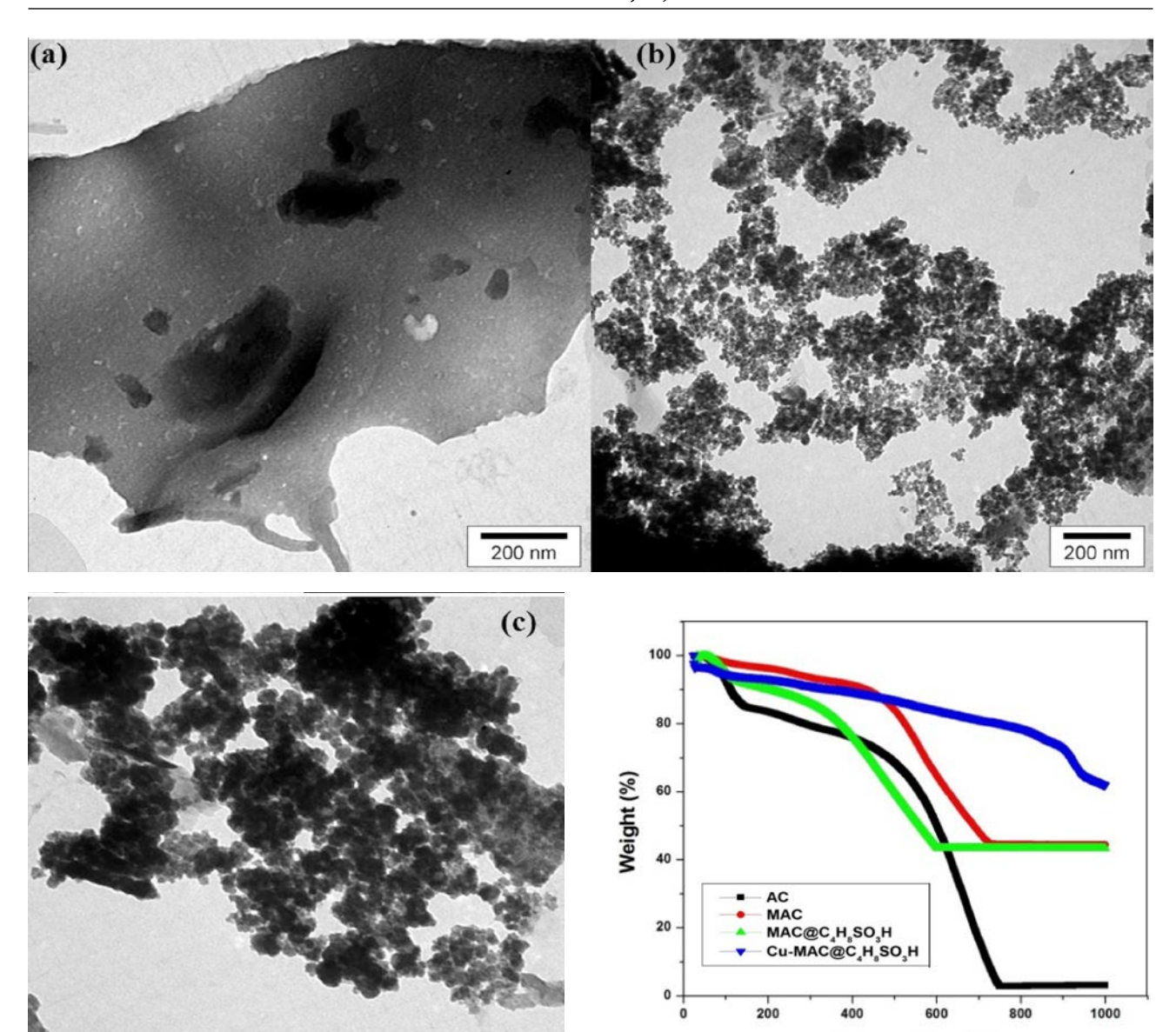


Figure 3. TEM images of, (a) AC (b) MAC (c) MAC@C $_4$ H $_8$ SO $_3$ H NCs.

Figure 4. TGA plots of (a) AC, (b) MAC (c) MAC@C $_4$ H $_8$ SO $_3$ H and (d) Cu-MAC@C $_4$ H $_8$ SO $_3$ H NCs.

Temperature (°C)

950 °C, due to the residual of copper oxide and iron oxide (Figure 4d).

The magnetization curves of the MAC, MAC@ $C_4H_8SO_3H$ and $C_4H_8SO_3H$ NCs are exhibited in Figure 5. The saturation magnetization of the MAC and MAC@ $C_4H_8SO_3H$ NCs was 21.73 and 16.33 emu g⁻¹ respectively; showing that this decrease in saturation magnetization can be attributed to the loading of $C_4H_8SO_3H$ on the MAC. Also, the saturation magnetization of the Cu-MAC@ $C_4H_8SO_3H$ NCs was 14.23 emu g⁻¹. This observed decrease in magnetic property was due to the loading of copper onto the surface of MAC@ $C_4H_8SO_3H$ NCs.

The presence of Fe $_3$ O $_4$, sulfamic acid and copper groups on the AC surface was further confirmed by the EDS analysis of the MAC@C $_4$ H $_8$ SO $_3$ H and Cu-MAC@C $_4$ H $_8$ SO $_3$ H NCs (Figure 6).

3. 2. Catalytic Activity

The catalytic activity of Cu-MAC@C $_4$ H $_8$ SO $_3$ H NCs was evaluated by the C–S coupling reaction for the synthesis of aryl thioquinazoline derivatives. The reaction of 2-mercapto-3-phenylquinazolin-4(3H)-one and iodobenzene was chosen to optimize the conditions of reaction and the results are reported in Table 1. Our observations

200 nm

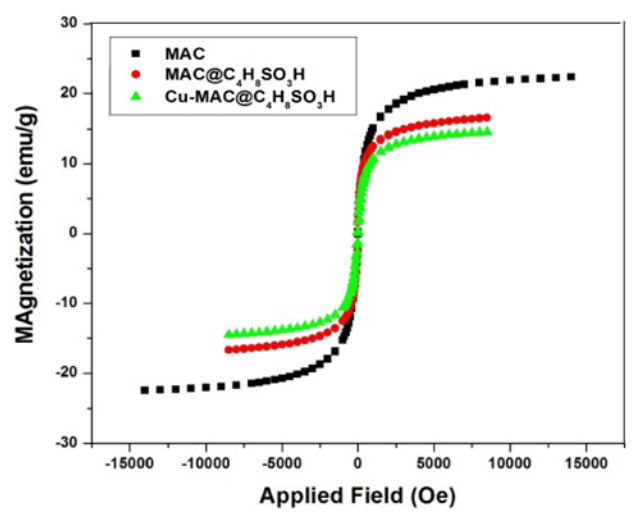


Figure 5. Magnetization curves of MAC, MAC@C $_4$ H $_8$ SO $_3$ H NCs and Cu-MAC@C $_4$ H $_8$ SO $_3$ H NCs.

showed that at this time the reaction had the same yield of 80% and therefore 4 hours was chosen as the optimal time for this reaction (Table 1, entries 4 and 5). Several solvent systems such as DMF, CH₃CN, dioxane, EtOH and H₂O were also tested and the high yield (80% yield) was obtained in DMF (Table 1, entries 6–9). In the next step, the reaction was performed in the presence of various bases such as K₂CO₃, Na₂CO₃, Et₃N, and NaOH among which K₂CO₃ had the best performance (Table 1, entries 4 and 10–12). Also, the reaction was tested in the presence of MAC and MAC@C₄H₈SO₃H NCs as the catalyst for 4 h and no product was detected, so the copper has the important catalytic role in this reaction (Table 1, entries 13 and 14).

According to the optimal conditions, capability and efficiency of Cu-MAC@C₄H₈SO₃H NCs were investigated in this reaction by screening different types of aryl halides and the results are presented in Table 2. In optimal condi-

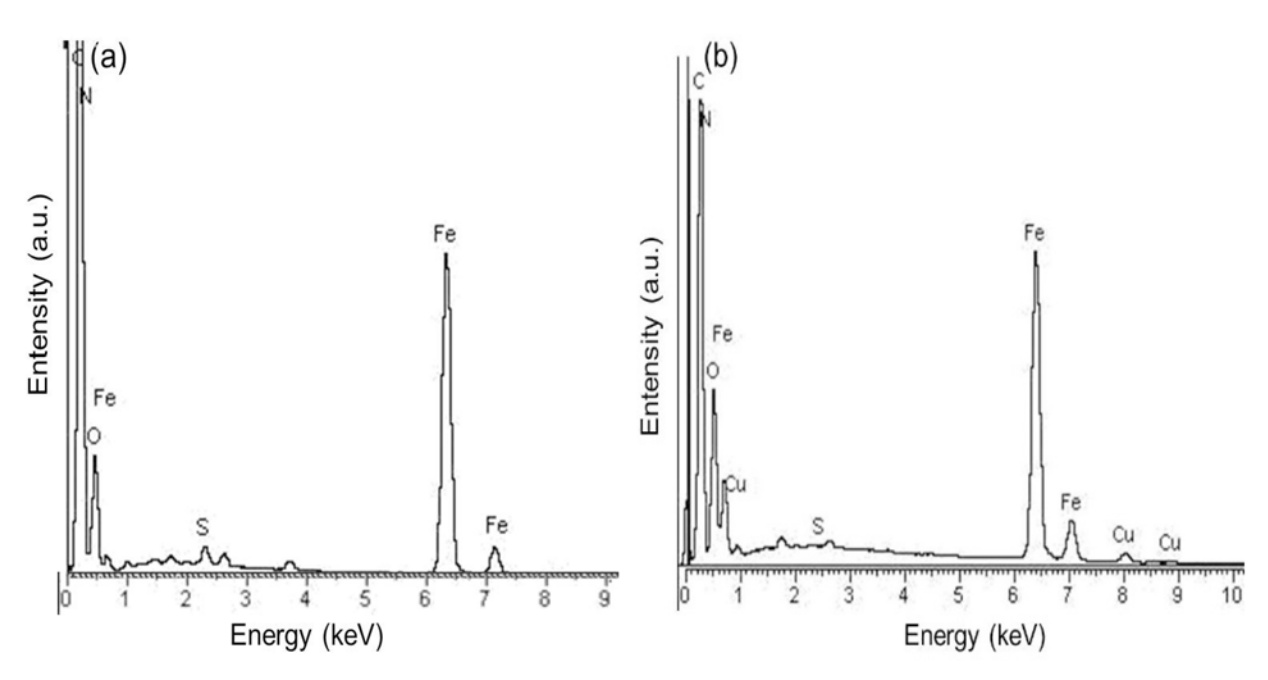


Figure 6. EDS pattern of (a) MAC@C₄H₈SO₃H NCs and (b) Cu-MAC@C₄H₈SO₃H NCs.

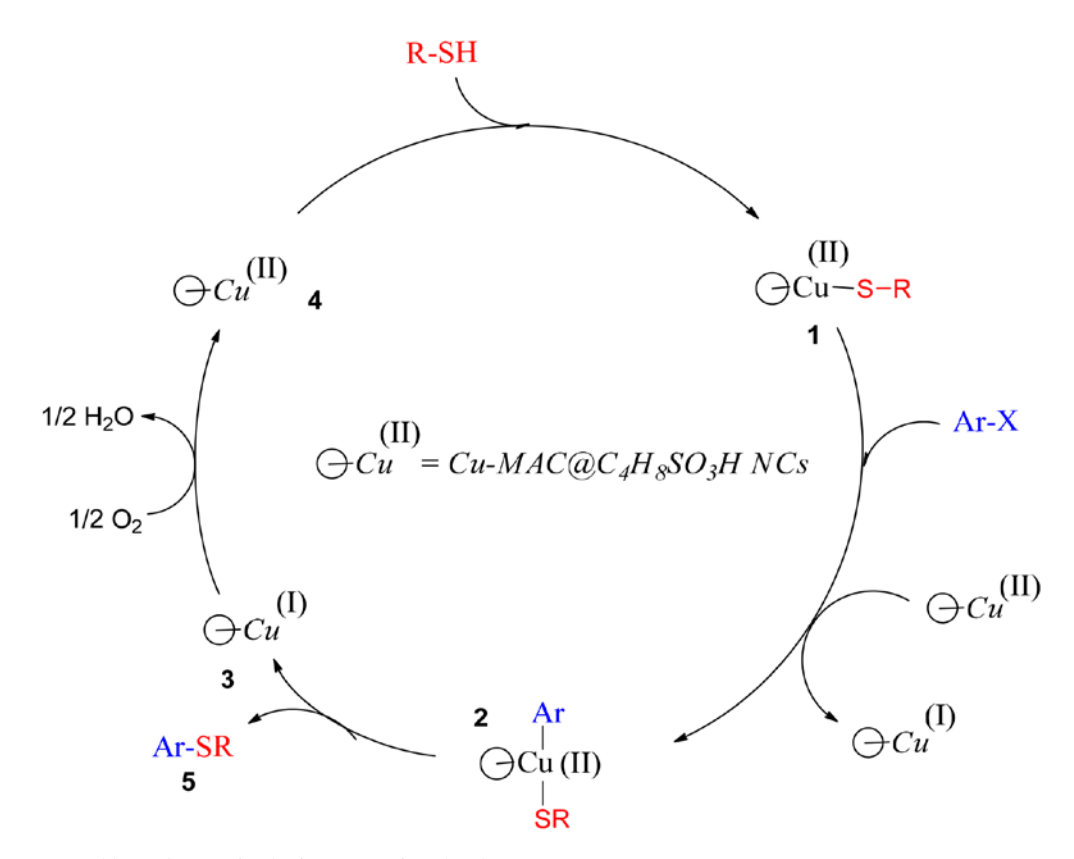
showed that the reaction carried out without catalyst was not successful under the following conditions: 2-mercapto-3-phenylquinazolin-4(3H)-one (a) (0.5 mmol, 0.127 g), iodobenzene (b) (0.5 mmol, 0.102 g) and 0.75 mmol (0.104 g) potassium carbonate as a base in 1.5 mL dimethylformamide (DMF) at 110 °C in closed vial for 2 h (Table 1, entry 1). This result confirmed that the catalyst has a vital role in this reaction. In next reaction, the MAC@ $C_4H_8SO_3H$ nanocomposites as a catalyst was added to the reaction mixture and only trace yield was observed, but by using Cu-MAC@ $C_4H_8SO_3H$ NCs the yield of reaction increased to 55% (Table 1, entries 2 and 3).

To investigate the effect of time on the reaction yield, the reaction was performed for 4 and 6 h, and the results tion, iodobenzene and bromobenzene were converted into the corresponding aryl thioquinazoline (**3a**) with 80 and 20% yields, respectively. In this reaction, aryl thioquinazoline was not formed when chlorobenzene was used instead of iodobenzene (Table 2, entries 1–3). The results showed that the methoxy (MeO) group in the *para* position of aryl halide could be effective and increase the yield of the product. For example, the isolated yields of aryl thioquinazoline from the reaction of 4-iodoanisol and 4-bromoanisol were 90 and 40%, respectively (Table 2, entries 4 and 5), while the yield of the corresponding product from 2-methoxyiodobenzene dropped to trace amounts (Table 2, entry 6). 3-Phenyl-2-(*para*-tolylthio)quinazolin-4(3*H*)-one (**3d**) was obtained from the reaction of 2-mercapto-3-phe-

 $\textbf{Table 1.} \ \ \textbf{Results of the C-S coupling reaction of 2-mercapto-3-phenylquinazolin-4(3H)-one and iodobenzene^a$

Entry	Catalyst	Solvent	Base	Time (h)	Yield ^b %
1	-	DMF	K ₂ CO ₃	2	0
2	MAC@C ₄ H ₈ SO ₃ H	DMF	K_2CO_3	2	trace
3	Cu-MAC@C ₄ H ₈ SO ₃ H	DMF	K_2CO_3	2	55
4	Cu-MAC@C ₄ H ₈ SO ₃ H	DMF	K_2CO_3	4	80
5	Cu-MAC@C ₄ H ₈ SO ₃ H	DMF	K_2CO_3	6	80
6	Cu-MAC@C ₄ H ₈ SO ₃ H	CH ₃ CN	K_2CO_3	4	50
7	Cu-MAC@C ₄ H ₈ SO ₃ H	Dioxane	K_2CO_3	4	15
8	Cu-MAC@C ₄ H ₈ SO ₃ H	EtOH	K_2CO_3	4	52
9	Cu-MAC@C ₄ H ₈ SO ₃ H	H_2O	K_2CO_3	4	0
10	Cu-MAC@C ₄ H ₈ SO ₃ H	DMF	Na_2CO_3	4	trace
11	Cu-MAC@C ₄ H ₈ SO ₃ H	DMF	Et ₃ N	4	5
12	CuMAC@C ₄ H ₈ SO ₃ H	DMF	NaOH	4	5
13	MAC	DMF	K_2CO_3	4	0
14	MAC@C ₄ H ₈ SO ₃ H	DMF	K_2CO_3	4	0

 $^{^{\}rm a}$ Reaction conditions: a (0.5 mmol), b (0.5 mmol), base (0.75 mmol), solvent (1.5 mL), catalyst (20 mg), 110 °C. $^{\rm b}$ Isolated yield.



 $\textbf{Scheme 2.} \ A \ reasonable \ mechanism \ for \ the \ formation \ of \ product \ by \ Cu-MAC@C_4H_8SO_3H \ NCs.$

Table 2. Synthesis of aryl thioquinazoline derivatives.^a

entry	Ar-X	product	yield ^b (g) ^c
1	Ç'	3a	80% (0.132 g)
2	Br	3a N S	20% (0.033 g)
3	CI	3a N S	0
4	e0 1	3b N S OMe	90% (0.162 g)
5	MeO Br	3b N S	40% (0.072 g)
6	OMe	3c N S OMe	Trace
7	Me	3d NNS	83% (0.143 g)
8	Me Br	3d N S Me	20% (0.034 g)
9	O ₂ N	3e NO2	94% (0.176 g)
10	Br	3f N S Br	74% (0.151 g)

 $[^]a$ Reaction conditions: arylhalide (0.5 mmol), 2-mercapto-3-phenylquinazolin-4(3*H*)-one (0.5 mmol), K₂CO₃ (0.75 mmol), DMF (1.5 mL), catalyst (20 mg), 110 °C for 4 h. b Isolated yield. c Yield as mass.

Nejadshafiee et al.: Copper and Magnetic Activated Carbon Nanocomposites: ...

nylquinazolin-4(3H)-one with 4-iodotoluene and 4-bromotoluene in 83 and 20% yields, respectively (Table 2, entries 7 and 8). Also, 2-((4-nitrophenyl)thio)-3-phenylquinazolin-4(3H)-one (3e) was formed in 94% yield from the reaction of 4-iodonitrobenzene under the optimal conditions (Table 2, entry 9). This result shows that the electron withdrawing (NO₂) group in the para position of iodobenzene can increase the yield of the mentioned product. In the final reaction, 4-iodobromobenzene was tested as the reactant and the corresponding product was isolated as 2-((4-bromophenyl)thio)-3-phenylquinazolin-4(3H)-one (3f) with 74% yield (Table 2, entry 10). All products were characterized by FT-IR, ¹H and ¹³C NMR spectroscopy and CHN analysis data (see supplementary material for details). According to the previous literature, the following reasonable mechanism can be suggested for this reaction (Scheme 2).^{30–32} In the first step of the mechanism transmetalation occurred to produce intermediate 1. In the next step, Ar-X is attached to the catalyst and an intermediate (II) is formed. This process continues by the oxidation and reduction of the copper cation and finally conversion to the coupled product 5 and copper(I) completes the catalytic cycle. In the cycle, oxidation of Cu(I) to Cu(II) is done by molecular oxygen from the atmosphere.

3. 3. Reusability of the Catalyst

The reusability of the catalyst was checked in the model reaction. After completion of the reaction and separation of the catalyst by using an external magnet, the composite was washed with DI water and ethyl acetate, dried under vacuum and reused in a subsequent reaction. As shown in Figure 7, there is only a slight decrease in the catalytic capacity after five cycles.

Reusability of Cat.

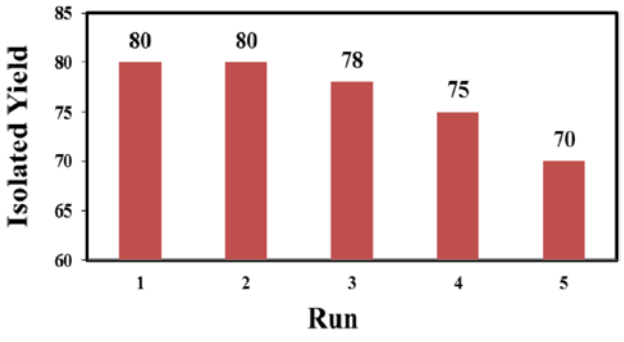


Figure 7. Reusability of Cu-MAC@C₄H₈SO₃H NCs in model reaction

4. Conclusions

In conclusion, we developed a nanocomposite as an efficient and reusable catalyst, which was prepared from activated carbon as solid phase with loading of copper and

magnetic nanoparticles (Cu-MAC@C₄H₈SO₃H NCs). The catalytic activity of the prepared nanocomposite was tested in a special C–S coupling reaction for the synthesis of aryl thioquinazoline derivatives in short times and high yields. In addition to the efficient and easy recycling, the catalyst can be used on a larger scale, making it a valuable candidate for practical applications.

Acknowledgments

We thank the Shahid Bahonar University of Kerman for financial support.

5. References

- R. A. Sheldon, Green Chem. 2016, 18, 3180–3183.
 DOI:10.1039/C6GC90040B
- P. J. Walsh, H. Li, C. A. Parrodi, Chem. Rev. 2007, 107, 2503– 2545. DOI:10.1021/cr0509556
- S. Yenice, C. Maden, N. Cakir, *Clinical Biochem.* 2009, 4, 333–342. DOI:10.1016/j.clinbiochem.2008.09.063
- 4. P. T. Anastas, J. C. Warner, Green Chemistry, "Green Chemistry" Frontiers 1998, 640, 1998–2002.
- K. Azizi, E. Ghonchepour, M. Karimi, A. Heydari, *Appl. Organometal. Chem.* 2015, 29, 187–194. DOI:10.1002/aoc.3258
- E. Ghonchepour, E. Yazdani, D. Saberi, M. Arefi, A. Heydari, *Appl. Organometal. Chem.* 2017, 54, 3822–3830.
 DOI:10.1002/aoc.3822
- E. Ghonchepour, M. R. Islami, T. A. Momeni, J. Org. Chem.
 2019, 883, 1–10. DOI:10.1016/j.jorganchem.2019.01.008
- F. Nikbakht, E. Ghonchepour, H. Ziyadi, A. Heydari, RSC Adv. 2014, 4, 34428–34435. DOI:10.1039/C4RA04911J
- E. Ghonchepour, D. Saberi, A. Heydari, *Org. Chem. Res.* 2017, 3, 44–49.
- H. Naeimi, V. Nejadshafiee, S. Masoum, RSC Adv. 2015, 5, 15006–15016. DOI:10.1039/C4RA17229A
- 11. H. Naeimi, V. Nejadshafiee, M. R. Islami, *B C S J.* **2016**, *89*, 212–219. **DOI**:10.1246/bcsj.20150291
- 12. H. Naeimi, V. Nejadshafiee, M. R. Islami, *Micropor. Mesopor. Mater.* **2016**, *227*, 23–30.
 - DOI:10.1016/j.micromeso.2016.02.036
- H. Naeimi, V. Nejadshafiee, New J. Chem. 2014, 38, 5429–5435. DOI:10.1039/C4NJ00909F
- P. G. Jessop, Syn. Org. Chem. Jpn. 2003, 61, 484–495.
 DOI:10.5059/yukigoseikyokaishi.61.484
- V. Nejadshafiee, M. R. Islami, *Mater. Sci. Eng. C.* **2019**, *101*, 42–52. **DOI:**10.1016/j.msec.2019.03.081
- M. M. Titirici, Sustainable carbon materials from hydrothermal processes, John Wiley & Sons 2013.
 DOI:10.1002/9781118622179
- V. Nejadshafiee, M. R. Islami, Environ. Sci. Pollut. Res. 2020, 27, 1625–1639. DOI:10.1007/s11356-019-06732-4
- V. Nejadshafiee, M. R. Islami, ChemistrySelect. 2020, 5, 8814–8822. DOI:10.1002/slct.202001801
- 19. F. Maghsoodi Goushki, M. R. Islami, V. Nejadshafiee, Mater.

- *Sci. Eng*: *B.* **2022**, *277*, 115591–115601. **DOI:**10.1016/j.mseb.2021.115591
- 20. E. Jafari, M. R. Khajouei, F. Hassanzadeh, G. H. Hakimelahi, G. A. Khodarahmi, *Res. Pharm. Sci.* **2016**, *11*, 1–14.
- 21. M. M. Ghorab, M. S. Alsaid, *Acta Pharma*. **2015**, *65*, 271–279. **DOI:**10.1515/acph-2015-0030
- 22. A. A. Radwan, F. K. Alanazi, M. H. Al-Agamy, *Braz. J. Pharm. Sci.* **2017**, *53*, 53–60.
- 23. S. Sangkharomaya, S. Nitayaphan, Research and Operational Support for the Study of Military Relevant Infectious Diseases of Interest to United States and Royal Thai Government; Armed forces research, Royal Thai Army Medical 2002. DOI:10.21236/ADA412783
- T. A. Ignatowski, R. N. Spengler, K. M. Dhandapani, R. F. H. Folkersma, Butterworth, E. Tobinick, CNS Drugs. 2014, 28, 679–697. DOI:10.1007/s40263-014-0174-2
- 25. C. B. Ahn, W. K. Jung, S. J. Park, Y. T. Kim, W. S. Kim, J. Y. Je, Gallic Acid-g-Chitosan Modulates Inflammatory Responses in LPS-Stimulated RAW264.7 Cells Via NF-κB, AP-1, and MAPK Pathways **2016**, *39*, 366–374.

- A. R. Khosropour, H. G. I. Mohammadpoor-Baltork, *Tetrahedron Lett.* 2006, 47, 3561–3564.
 DOI:10.1016/j.tetlet.2006.03.079
- E. R. Wood, A. T. Truesdale, O. B. McDonald, D. Yuan, A. Hassell, S. H. Dickerson, B. Ellis, C. Pennisi, E. Horne, K. Lackey, *Cancer Res.* 2004, 64, 6652–6659.
 DOI:10.1158/0008-5472.CAN-04-1168
- E. Raymond, S. Faivre, J. P. Armand, Drugs. 2000, 60, 15–23.
 DOI:10.2165/00003495-200060001-00002
- 29. T. J. Lynch, D. W. Bell, R. Sordella, S. Gurubhagavatula, R. A. Okimoto, B. W. Brannigan, P. L. Harris, S. M. Haserlat, J. G. Supko, F. G. Haluska, *NEJM*. **2004**, *350*, 2129–2139. **DOI:**10.1056/NEJMoa040938
- 30. N. A. Dangroo, T. Ara, B. A. Dar, M. Khuroo, *Catal Commun.* **2019**, *118*, 76–80. **DOI**:10.1016/j.catcom.2018.10.006
- C. Sambiagio, S. P. Marsden, A. J. Blacker, P. C. McGowan, *Chem. Soc. Rev.* **2014**, 43, 3525–3550.
 DOI:10.1039/C3CS60289C
- 32. A. Casitas, X. Ribas, *Chem. Sci.* **2013**, *4*, 2301–2318. **DOI:**10.1039/c3sc21818j

Povzetek

DOI:10.1007/s10753-015-0258-2

V tej študiji smo aktivno oglje (AC) pripravili iz lupin pistacij kot kmetijskega odpadka. Pripravljeno aktivno oglje smo uporabili kot nosilec za vezavo bakrovih in magnetnih nanodelcev in tako sintetizirali učinkovite nanokompozite (Cu-MAC@C $_4$ H $_8$ SO $_3$ H NC). Strukturo nanokatalizatorja smo določili z različnimi metodami, vključno z FT-IR, TEM, EDS, XRD, VSM in TGA analizami. Katalitsko aktivnost pripravljenih kompozitov smo preverili na primeru posebnega C–S spajanja med 2-merkapto-3-fenilkinazolin-4(3H)-onom in jodo- oz. bromobenzenom. Po kratkih reakcijskih časih smo z dobrimi izkoristki kot produkte izolirali derivate aril tiokinazolinov. Produkte smo karakterizirali s pomočjo 1 H, 13 C NMR in CHNS elementnih analiz. Ker je recikliranje katalizatorja Cu-MAC@C $_4$ H $_8$ SO $_3$ H na osnovi njegovih magnetnih lastnosti enostavno in učinkovito, smo torej prikazali zeleni pristop k povečanju aktivnosti nanokatalizatorjev. Nanokatalizatorje smo uporabili v petih ciklih in ob tem ni prišlo do opaznega zmanjšanja aktivnosti.